Available online at www.sciencedirect.com
ScienceDirect
Journal of Nuclear Materials 358 (2006) 217–226
journal of nuclear materials
www.elsevier.com/locate/jnucmat

Intrinsic martensite formation in neutron irradiated V–1.6%Y alloys with fine-grained structure of highly pure matrix

H. Kurishita [a,*], S. Kobayashi [b], K. Nakai [b], T. Kuwabara [c,1], M. Hasegawa [a]

[a] *International Research Center for Nuclear Materials Science, Institute for Materials Research (IMR), Tohoku University, Oarai, Ibaraki 311-1313, Japan*
[b] *Department of Materials Science and Engineering, Ehime University, Matsuyama 790-8577, Japan*
[c] *Graduate Course Student, International Research Center for Nuclear Materials Science, IMR, Tohoku University, Oarai, Ibaraki 311-1313, Japan*

Received 18 March 2006; accepted 18 July 2006

Abstract

Effects of neutron irradiation were examined on microstructural evolution in powder metallurgically processed V–1.6Y (in wt%) alloys comprising essentially fine grains and very fine dispersoids of Y_2O_3 and YN. The alloys feature a highly pure matrix free from gaseous interstitials such as oxygen and nitrogen. Optical and transmission electron microscopy observations revealed that the martensite of a vanadium bct structure with a tetragonality (c/a) of 1.06 formed heterogeneously in some of the bcc grains of V–1.6Y irradiated at 290 and 600 °C to 0.25 and 0.6 displacement per atom, respectively, but not in unirradiated V–1.6Y. The martensite had $\{1\,0\,1\}_{bct}$ habit planes parallel to $\{1\,1\,0\}_{bcc}$ in the matrix and a high density of $\{1\,0\,1\}_{bct}$ microtwins as the lattice invariant shear strain. To the authors' knowledge, the emergence of martensite is the first to be observed for vanadium or its alloys in neutron irradiated states. The cause of the martensite formation is discussed.

PACS: 28.52.Fa; 62.20.Mk

1. Introduction

Vanadium and its alloys are attractive candidate materials for fusion reactor structural applications because of their inherently low-induced activation characteristics, large thermal stress factor and high fracture toughness before irradiation [1–3]. In order to make the alloys more attractive, it is necessary to improve the resistance to embrittlement by high-energy particle irradiation [4,5].

* Corresponding author. Tel.: +81 29 267 4157; fax: +81 29 267 4947.
E-mail address: kurishi@imr.tohoku.ac.jp (H. Kurishita).
[1] Present Address: Electronics and Materials R&D Laboratories, Sumitomo Electric Industries, Ltd. Osaka Works, 1-1-3, Shimaya, Konohana-ku, Osaka 554-0024, Japan.

0022-3115/$ - see front matter © 2006 Elsevier B.V. All rights reserved.
doi:10.1016/j.jnucmat.2006.07.016

The most effective microstructure to alleviate radiation embrittlement consists of fine grains and finely dispersed particles, the finer the better because grain boundaries and particles can serve as effective sinks for irradiation induced point defects. Such a microstructural refinement in vanadium requires advanced powder metallurgical (P/M) methods that enable to make the vanadium matrix free from gaseous interstitials, particularly nitrogen and oxygen. This is because vanadium is very chemically reactive with the interstitials and their dissolution into the matrix leads to significant embrittlement. The authors proposed such an advanced P/M method utilizing mechanical alloying (MA) [6] and hot isostatic pressing (HIP) and developed V–Y, V–Y–Ti, V–Y–Cr and V–Y–W alloys with the desired microstructures [7–11]. The developed alloys exhibited very fine, high-purity grains and very fine dispersoids of Y_2O_3 and YN as a result of consuming solute oxygen and nitrogen impurities to form Y_2O_3 and YN. By using the alloys, the effects of neutron irradiation on microstructural evolution and Vickers microhardness were examined [8,12,13]. Since structural applications of the alloys require sufficient mechanical properties prior to irradiation as well, the effects of grain size and dispersion parameters on room and/or high temperature tensile properties of the V–Y, V–Y–Ti, V–Y–Cr, V–Y–W and V–Y–Ti–Mo alloys were studied [8–11,14–16].

Our previous papers concerning neutron irradiation effects showed that twin-like microstructures are observed in V–1.6 wt%Y irradiated with fast neutrons at 290 and 600 °C to 0.25 and 0.6 displacement per atom (dpa), respectively [12]. However, the details of the twin-like microstructures have not been reported so far.

In this paper, transmission electron microscopy (TEM) examinations of the twin-like microstructures in the irradiated V–1.6 wt%Y alloys were conducted. It is shown that the twin-like microstructures are the bct {1 0 1) microtwins that are the lattice invariant shear strain in a martensite lath with habit planes of $\{1\,0\,1\}_{bct}\|\{1\,1\,0\}_{bcc}$. The tetragonality ($c/a$) of the martensite lattice is 1.06.

2. Experimental

Powders of pure vanadium (particle size: <150 μm, oxygen: 0.08 wt%, nitrogen: 0.07 wt%) and pure yttrium (<750 μm, 1.56 wt%, 0.05 wt%) were used as the starting materials. They were mixed to provide a nominal composition of V–1.6Y (in wt%) in a glove box filled with a purified Ar gas (purity 99.99999%). The mixed powder was charged into two vessels made of WC/Co and sealed with an oxygen-free copper gasket in the glove and then subjected to MA with a planetary ball mill (model:Fritch P 5) in the purified Ar atmosphere. In order to obtain a microstructure where most of the grains are fine, whereas a fraction of the grains remain coarse, slightly MA treated powders of vanadium were blended into the fully MA treated powders of V–1.6Y. Such a microstructure is advantageous to clarify the effects of grain size on microstructural evolution developed under the identical irradiation condition. The blended powders were enclosed in a mild steel capsule (about 35 mm in diameter and 53 mm in height), which was TIG weld sealed after outgassing. HIP was conducted at 800 and 1000 °C and 196 MPa for 3 h in an Ar atmosphere. The density of the as-HIPed compacts was 6.09 g/cm^3, approximately 99.5% of theoretical value.

From the as-HIPed compacts, specimens for TEM microstructural observations and X-ray diffraction (XRD) analyses were prepared. All of the specimens were wrapped with Ta foil and then Zr foil and annealed at 1000 °C for 1 h in a vacuum better than 5×10^{-5} Pa. Table 1 shows the designations and chemical compositions of the specimens. Here, V–1.6Y-1 was HIPed at 800 °C and V–1.6Y-2 at 1000 °C. The post HIP annealing at 1000 °C for 1 h, however, resulted in almost the same average grain size in the fine-grained area, 290 nm for V–1.6Y-1 and 303 nm for V–1.6Y-2 [8]. The yttrium content of 1.56 wt% is excessive by approximately 0.4% with respect to the stoichiometry of Y_2O_3 and YN so that all the oxygen and nitrogen in Table 1 can be consumed to form Y_2O_3 and YN. The contents of tungsten and Ar arising from the milling vessels/balls and the atmosphere, respectively, during MA are also shown.

XRD analyses using Cu K_α radiation were made to identify the microstructures including dispersed compound particles under the conditions of 30 kV and amperage of 250 mA.

Table 1
Chemical compositions of specimens (wt%)

Specimen	O	N	C	H	Y	W	Ar
V–1.6Y-1	0.171	0.078	0.0249	0.0004	1.56	0.02	0.0014
V–1.6Y-2	0.141	0.075	0.0222	0.0004	1.56	0.09	0.0012

Neutron irradiation was performed in a helium atmosphere to fluences of 1.3×10^{24} n/m^2 (about 0.25 dpa) at 290 °C for V–1.6Y-1 and 3.7×10^{24} n/m^2 (about 0.6 dpa) at 600 °C for V–1.6Y-2 in the Japan Materials Testing Reactor (JMTR).

Thin foils for TEM were prepared by twin-jet electropolishing using a solution of 20 vol% H_2SO_4 and 80 vol% C_2H_5OH around 0 °C at 20 V and also by focused ion beam (FIB) techniques without electropolishing, and examined in JEM2000FX and JEM4000EX microscopes operating at 200 and 400 kV, respectively.

3. Results

It was confirmed that the microstructures of V–1.6Y-1 and V–1.6Y-2 were comprised of fine (about 0.3 μm) and coarse grains (about 30 μm); most of the grains remained fine and coarse-grained areas were sparsely distributed and surrounded by the fine-grained areas. The coarse grains are derived from the slightly MA treated powders and contain very few dispersoids because of the absence of yttrium supersaturated in the matrix by MA [8]. The Vickers microhardness selectively measured at the coarse-grained areas was very low ($HV = 56 \pm 9$ [8]). This indicates that the coarse-grained areas can be considered to be free from solute nitrogen and oxygen which are consumed to form dispersoids of Y_2O_3 and YN [8]: Solute nitrogen and oxygen impurities in the coarse-grained areas can diffuse over sufficient distance to bind supersaturated yttrium existing in the surrounding fine-grained areas during HIPing and subsequent annealing. XRD analyses for the HIPed and annealed specimens revealed distinct diffraction peaks by Y_2O_3 and YN, which are due to the reaction of solute oxygen and nitrogen with yttrium [7–9].

Fig. 1 shows surface reliefs observed in the coarse-grained areas in V–1.6Y-1 and V–1.6Y-2 irradiated at 290 °C to 0.25 dpa and at 600 °C to 0.6 dpa, respectively. If the observed surface reliefs are formed by {1 1 2} twinning in the bcc vanadium matrix, the surface reliefs should exist nearly along 12 directions. However, careful examinations of Fig. 1 show that the surface reliefs in a grain comprise only 3–5 different directions. In view of the

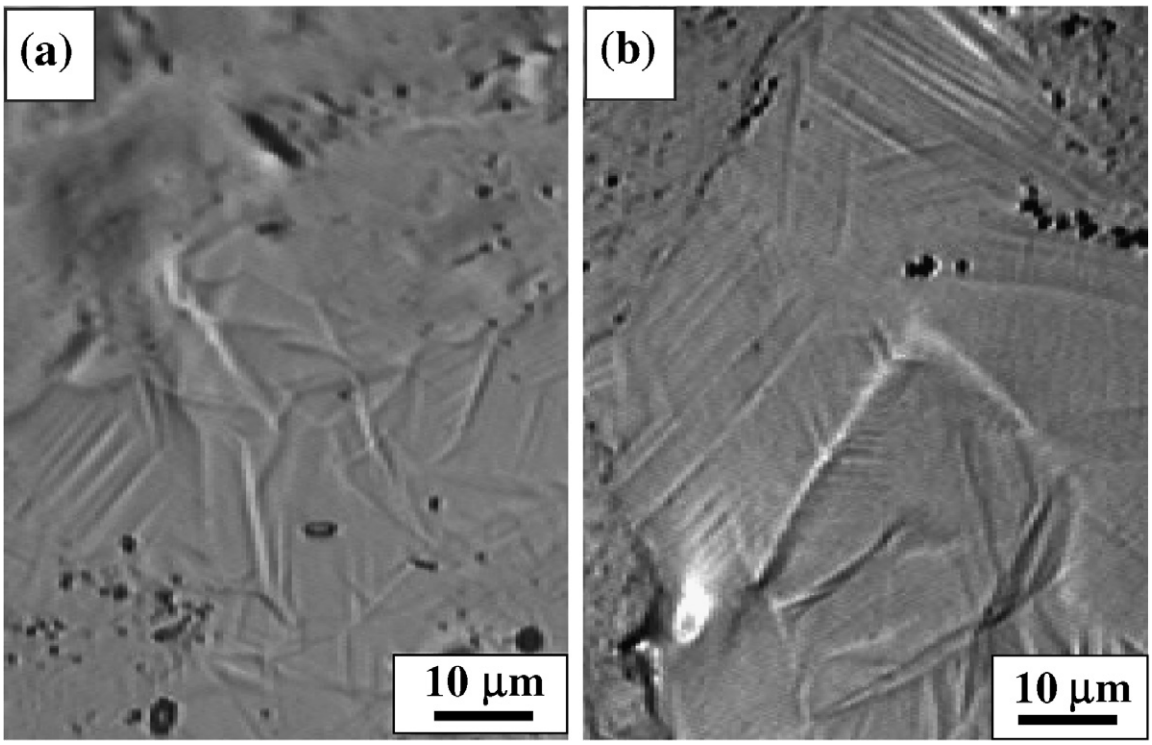

Fig. 1. Surface reliefs in the coarse-grained areas in (a) V–1.6Y-1 irradiated at 290 °C to 0.25 dpa and (b) V–1.6Y-2 irradiated at 600 °C to 0.6 dpa.

occurrence of such sharp large reliefs at a lower irradiation temperature of 290 °C, it is likely that the reliefs were produced by diffusionless processes. The observed surface reliefs are due to the lattice displacement of a fixed vector in the every fixed lattice planes.

Fig. 2 shows a TEM micrograph of a transformed region taken from the electropolished specimen of V–1.6Y-1 irradiated at 290 °C to 0.25 dpa. A number of microtwins are observed in the region. Such transformed regions emerged heterogeneously in some of the fine grains or some part of the coarse-grained areas. Diffraction pattern analyses of Fig. 2(c) showed that the pattern was well indexed as a bct phase with an ordered arrangement of hydrogen atoms in the vanadium bct lattice.

In view of the aspect that irradiated materials contain a high density of trapping sites for hydrogen atoms, the microstructures of the irradiated specimens likely inhibit particular arrangements of hydrogen or formation of a hydride without the existence of highly concentrated hydrogen in a thin area of the specimen. The possible source of such concentrated hydrogen may be due to pickup associated with electropolishing for TEM specimen preparation after irradiation: the hydrogen content in the as-prepared specimens prior to irradiation was only 0.0004 wt% (H/V = 0.0002, Table 1) and the irradiation atmosphere was He. However, TEM images obtained from a FIB-polished specimen without electropolishing exhibited microtwins similar to Fig. 2(a). Therefore, it is reasonable to state that the observed bct phase was formed in the following way: a bct phase *of vanadium* was first formed by neutron irradiation, and then picked-up hydrogen atoms were placed with an ordered arrangement in the vanadium bct phase that can provide preferential sites for hydrogen even in the irradiated specimens with a high density of hydrogen trapping sites. In fact, Fig. 2 was obtained for *a very thin* specimen area that is susceptible to hydrogen pickup associated with TEM specimen preparation after irradiation, as seen from the existence of a hole in Fig. 2(a): the hole was formed by electropolishing for TEM specimen preparation. In order to verify these arguments and evaluate the tetragonality (c/a) of the bct phase, TEM examinations were conducted on a *thicker area* in the electropolished specimen so that the observed results can reflect the *intrinsic structures* which are not essentially influenced by hydrogen pickup.

Fig. 3 shows a bright field image exhibiting microtwins and a selected area diffraction (SAD) pattern for a thicker specimen area in V–1.6Y-2 irradiated at 600 °C to 0.6 dpa. In the SAD pattern (Fig. 3(b)) the angle between the $(0\,1\,-1)$ and $(0\,-1\,-1)$ planes is 94°, which indicates the existence of a bct phase in the observed thicker area. It should be here noted that the SAD pattern does not contain the diffraction spots derived from the ordered hydrogen arrangement as shown in Fig. 2(c), but is well indexed as the vanadium bct phase. It is obvious that the bct vanadium phase formed independently of hydrogen pickup associated with specimen preparation after irradiation.

In Fig. 3(c) several pairs of Kikuchi lines are indexed by using a calculated Kikuchi map. Interspacing of pairs of the Kikuchi lines yields a tetragonality value of 1.06. Assuming that this value of 1.06 is also applicable to the tetragonalily of the bct phase in Fig. 2, it equates the atomic ratio of H/V to approximately 0.24 [17]. This ratio is much smaller than H/V = 0.41, the lowest ratio of the β_1 hydride phase that can exist in the thermoequilibrium state [18], supporting the absence of hydride formation in the bct phase. The transformed vanadium bct lattice provided preferential sites as the host phase for picked-up hydrogen atoms to occupy with an ordered arrangement even in the irradiated specimens.

In conclusion, the observed bct phase with $\{1\,0\,1\}$ twin boundaries occurred by martensitic transformation, independently of hydrogen pickup. The $\{1\,0\,1\}$ microtwins are most likely due to the lattice invariant shear strain required to accommodate the transformation strain induced in the martensite of the bct structure formed by irradiation. Hereafter, we will use the expression of bct martensite or martensite of a bct structure.

The determination of the habit plane of the martensite in the matrix is important. As suggested from the surface reliefs in Fig. 1, the lath width of martensite often exceeds the diameter of the fine grains. Fig. 4 shows an example of the interface observed in a coarse grain in V–1.6Y-2 irradiated at 600 °C to 0.6 dpa. The interface is marked with a solid line at which two martensite-variants encountered. The interface is seen to be parallel to the twin boundaries in the upper half of Fig. 4. In order to confirm that the two dotted lines marked in Fig. 4 correspond to the bct $\{1\,0\,1\}$ twin boundaries of the lattice invariant strain, the angle between the two intersecting dotted lines was

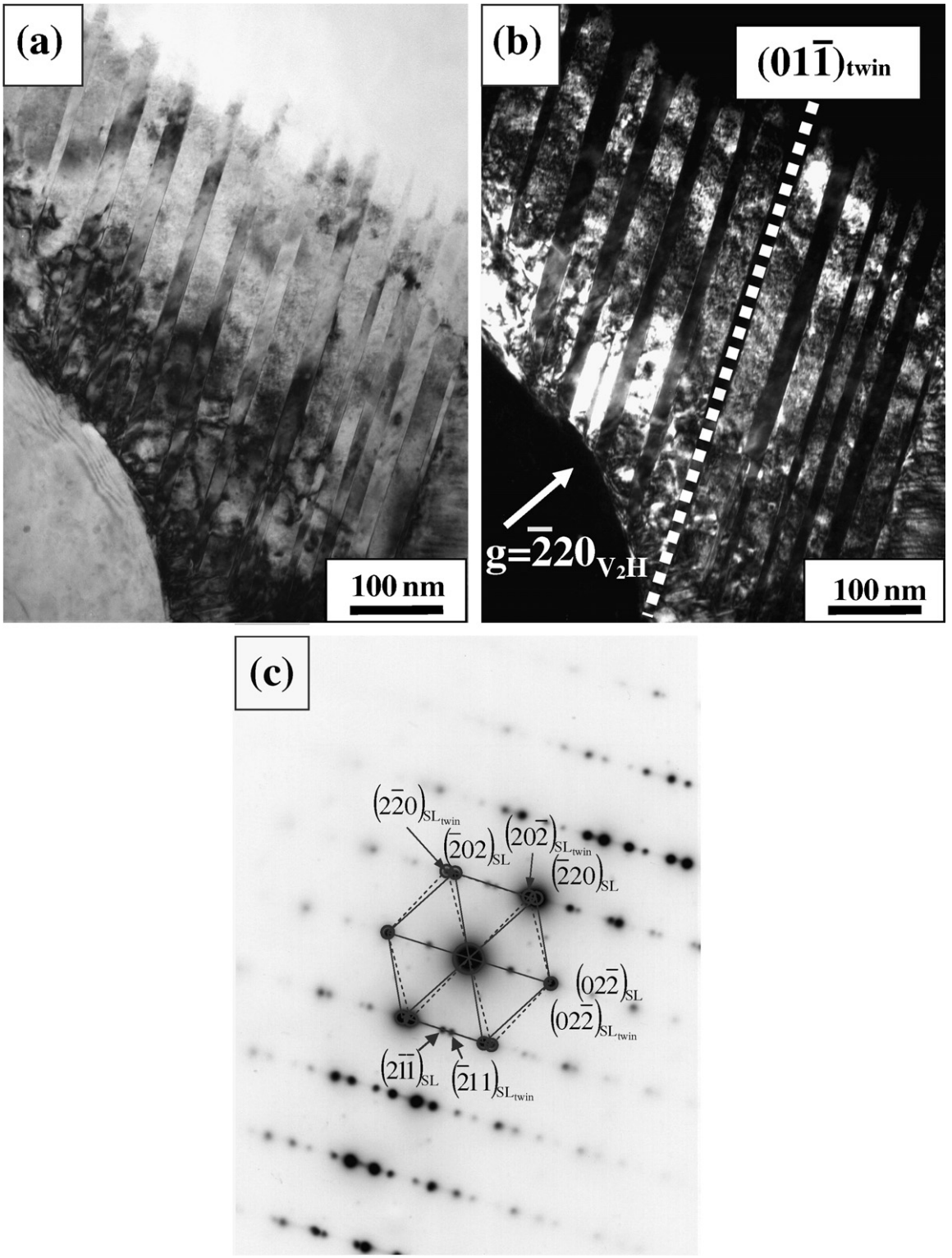

Fig. 2. TEM micrographs of (a) bright field and (b) dark field images and (c) selected area diffraction pattern from a very thin specimen area with a transformed region in V–1.6Y-1 irradiated at 290 °C to 0.25 dpa. A high density of {1 0 1} microtwins are observed. SL represents super lattice spots due to an ordered arrangement of hydrogen atoms in the vanadium bct lattice.

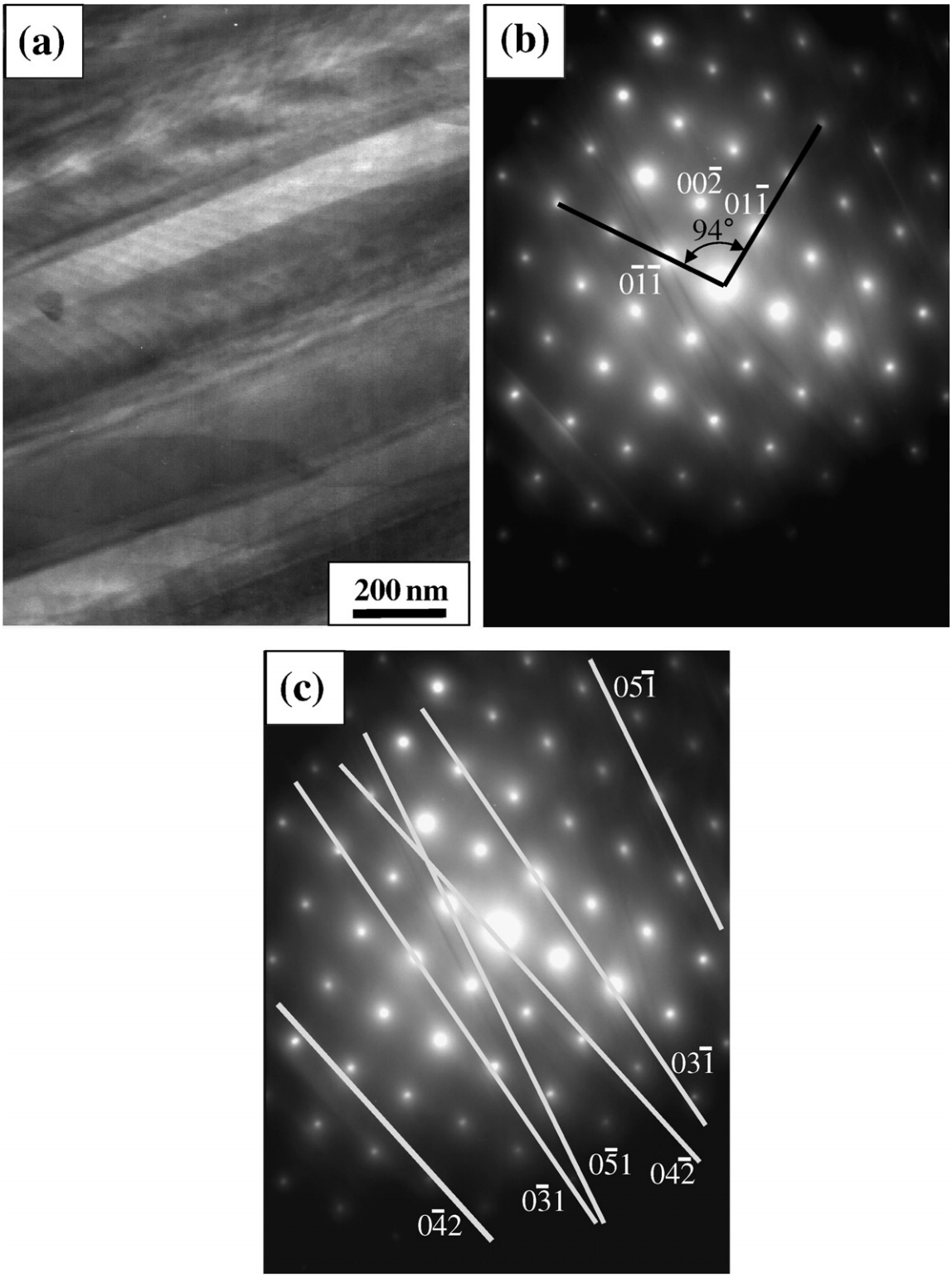

Fig. 3. (a) TEM bright field image exhibiting microtwins, (b) selected area diffraction pattern and (c) several pairs of Kikuchi lines indexed, obtained from a thicker specimen area with a transformed region that is considered almost insusceptible to picked-up hydrogen in V–1.6Y-2 irradiated at 600 °C to 0.6 dpa. Kikuchi line analyses give a tetragonality of 1.06.

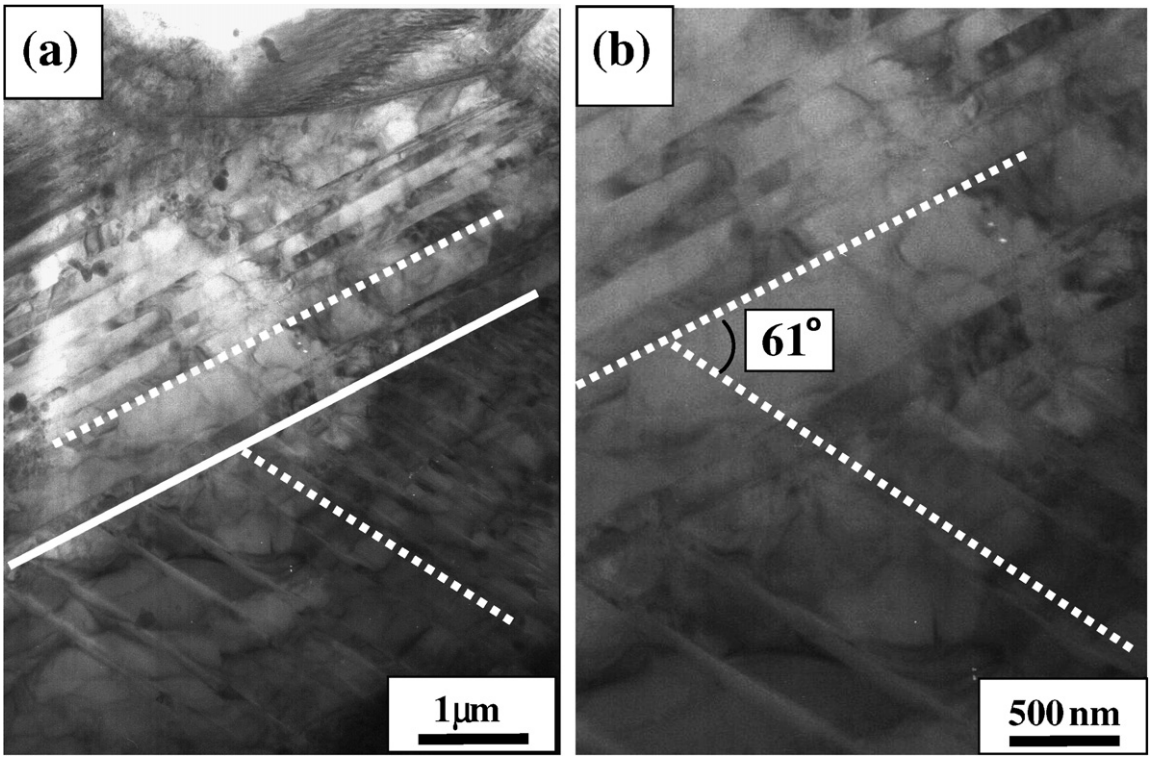

Fig. 4. An interface between a twinned bct martensite and the surrounding bcc matrix in a coarse grain in V–1.6Y-2 irradiated at 600 °C to 0.6 dpa. The interface is marked with a solid line at which two martensite-variants encounter. The dotted lines are twin boundaries in different variants that encounter.

precisely measured. The angle deviated from 60°, which can be explained by assuming the (1 0 1) and (0 1 1) twin boundaries in the bct phase with the tetragonality of approximately 1.06. Other examples of the interfaces are shown in Fig. 5 for the martensite formed in fine grains in V–1.6Y-2. The interfaces marked by the dotted lines are parallel to the twin boundaries. From these results we can say that the interface between the martensite-variant and bcc matrix, i.e., the habit plane of the bct martensite, is $\{1\,0\,1)_{bct}\|\{1\,1\,0\}_{bcc}$.

4. Discussion

In this study the martensite with habit planes of $\{1\,0\,1)_{bct}\|\{1\,1\,0\}_{bcc}$ was identified in V–1.6Y-1 and V–1.6Y-2 irradiated with neutrons at 290 and 600 °C to 0.25 and 0.6 dpa, respectively, but not identified in the unirradiated specimens. This indicates that the occurrence of martensite with bct structure in the bcc matrix was caused by irradiation. To the authors' knowledge, the emergence of martensite formation in vanadium or its alloys after neutron irradiation is the first to be detected, though extensive studies on the effects of irradiation on microstructural evolution in vanadium and its alloys have been conducted so far. The reason for the inducement of martensite is discussed below.

It is well-known that in vanadium gaseous interstitials such as oxygen cause the transformation from the bcc to bct structure by elongating one axis relative to the other two to accommodate the induced strain [19]. After Hiraga et al., up to the atomic ratio of oxygen to vanadium (O/V) of 0.07 (approximately 2.0 wt%) the bcc structure of vanadium is maintained, but above 0.07 the lattice constant is increased and the bcc changes to the bct structure over the whole area of the specimens by martensitic transformation. The bct structure exhibits the tetragonality of approximately 1.03 and above [19], and the value of 1.06 obtained for the present irradiated specimens is in this range. However, the cause of the martensite formation observed in this study is considered to be different from oxygen dissolution into the vanadium matrix, as discussed below.

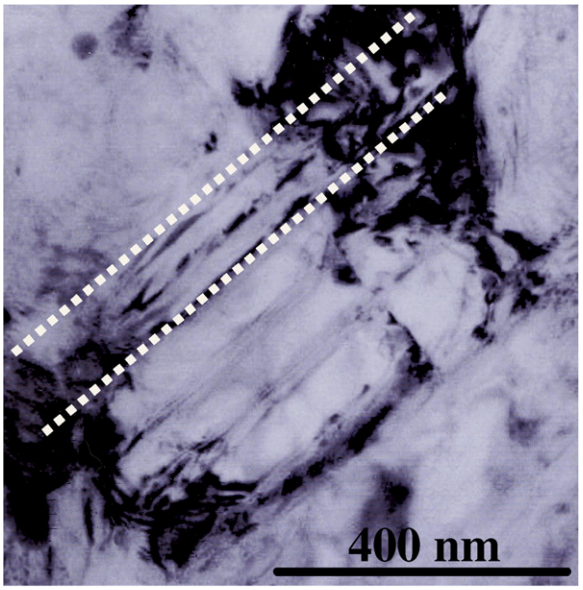

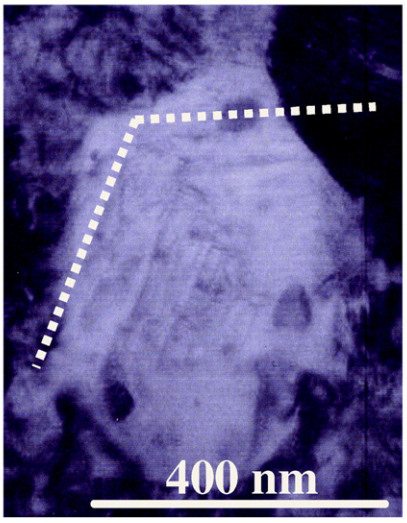

Fig. 5. TEM bright-field images showing the interfaces of martensite formed in fine grains in V–1.6Y-2 irradiated at 600 °C to 0.6 dpa. The interfaces marked by dotted lines are parallel to the twin boundaries.

1. As observed in this study, the transformation from the bcc to bct phase did not occur over the whole areas of grains in the alloys, but occurred heterogeneously in some of the fine grains or some part of the coarse-grained areas. This indicates that the explanation of the observed transformation in terms of oxygen dissolution requires a very heterogeneous distribution of solute oxygen with the maximum concentration above 2.0 wt%. However, such a heterogeneous distribution of solute oxygen is unrealistic.
2. The oxygen contents in the alloys shown in Table 1 were 0.14 and 0.17 wt%, which are much lower than 2.0 wt%. In view of the fact that oxygen impurities reacted with yttrium atoms and formed thermally stable Y_2O_3 during HIP and subsequent annealing, the residual content of solute oxygen in the vanadium matrix is negligibly small [7–9]. Even if a heterogeneous distribution of solute oxygen mentioned above *were likely*, the residual content of solute oxygen should be by far lower than that required for the phase transformation suggested by Hiraga et al.
3. The possibility of pick-up of oxygen and/or nitrogen from the surroundings during JMTR irradiation can be excluded because no appreciable increase in the Vickers microhardness due to irradiation at 290 and 600 °C was observed for the fine-grained areas in the TEM specimens; HV = 195 and 203 before and after irradiation at 290 °C in V–1.6Y-1, and 183 and 199 before and after irradiation at 600 °C in V–1.6Y-2, respectively [8]. In addition, no appreciable increase in the amount of dispersoids, which may be formed by the reaction of the picked-up oxygen and/or nitrogen, if any, with free yttirum atoms of approximately 0.4 wt% in V–1.6Y-1 and V–1.6Y-2, was recognized after irradiation.

As described previously, the characteristics of the P/M processed V–1.6Y-1 and V–1.6Y-2 alloys are essentially fine grains and highly pure matrix free from interstitial impurities. Such a fine-grained structure with an interstitial-scavenged matrix, which has not been available by conventional processing such as melting techniques, is likely to be responsible for the occurrence of the martensite in the irradiated P/M V–1.6Y alloys, as discussed below.

Neutron irradiation is known to cause a high density of cascades, which lead to depleted zones, isolated self interstitial atoms (SIA) and vacancies, etc. SIAs preferentially flow to sink sites such as grain boundaries, dislocations and interface boundaries between dispersed particles and the matrix, and add new lattice sites around the sink sites. Providing that SIAs do not recombine with vacancies to annihilate, all of the remained defects, especially SIAs occupying the additional lattice sites, cause a strain field in the grain interior *under the elastic constraint* by the surrounding grain boundaries. In the

highly elastically strained grains the bcc structure tends to be destabilized so that martensitic transformation is inclined to occur from the bcc to bct structure. The fine-grained structure receives a larger elastic constraint and also can be more self-accommodating because of smaller martensite plate sizes than the coarse-grained structure. On the other hand, in the coarse grains of V–1.6Y-1 and V–1.6Y-2 the elastic constraint can also be induced because the coarse grains were scarcely distributed and surrounded by the fine-grained areas, which may cause strain in the coarse-grain interior by irradiation.

The occurrence of the bct martensite in the bcc matrix requires the formation and extension of the bcc/bct interfaces. Since the extension of the interfaces accompanies movement of the interface dislocations, the high purity matrix of V–1.6Y-1 and V–1.6Y-2 and good coherency between the martensite and the matrix may lead to the enhancement of movements of the interface dislocations and twin shearing. The habit planes, $\{1\,0\,1\}_{bct}\|\{1\,1\,0\}_{bcc}$, can be regarded as the lowest energy and close-packed plane of both the structures because the lattice constants of both the phases are almost the same.

The observed heterogeneous occurrence of the martensite in both of the fine- and coarse-grains in V–1.6Y-1 and V–1.6Y-2 can be a reflection of heterogeneous distributions of the resultant strains accumulated in the specimens by irradiation. The heterogeneity is mainly attributable to the distribution of sink sites in the as-fabricated state of V–1.6Y-1 and V–1.6Y-2, which is influential in the strain field built up in the grains under a given irradiation condition.

The above explanation concerning the occurrence of martensite does not mean that only irradiation causes martensite formation in vanadium alloys, although a bct phase and surface reliefs were not observed in the unirradiated specimens of V–1.6Y-1 and V–1.6Y-2. Any causes that can introduce a large degree of strain in bcc vanadium matrices can be regarded as a potential trigger for martensite formation. It can be hence argued that providing that the grains are fine enough to be elastically constrained and subjected to a large degree of induced strain and that the matrix is highly pure, martensite formation is a possible consequence to occur and the transformed bct phase with {1 0 1} microtwins may be observed even in the unirradiated state.

5. Conclusions

1. The twin-like microstructures observed in the V–1.6Y-1 and V–1.6Y-2 alloys irradiated with neutrons at 290 and 600 °C to 0.25 and 0.6 dpa, respectively, are identified to be bct {1 0 1} microtwins.
2. The $\{1\,0\,1\}_{bct}$ microtwins are the lattice invariant shear strain of martensite with a bct structure transformed from the bcc matrix. The bct structure has a tetragonality (a/c) of 1.06 as measured with Kikuchi line analyses.
3. The habit planes between the bct martensite and the surrounding bcc matrix are $\{1\,0\,1\}_{bct}\|\{1\,1\,0\}_{bcc}$, which can be regarded as the close-packed plane with coherency even for the bct structure because of the slight changes in the lattice constants of both the phases.
4. The occurrence of martensite for vanadium or its alloys in the neutron irradiated states is, to the authors' knowledge, the first to be observed. The features of the P/M V–1.6Y alloys, an interstitial-scavenged matrix and extremely fine grains, are considered to be responsible for the martensite formation caused by irradiation.
5. An ordered arrangement of hydrogen atoms in the vanadium bct lattice occurs in *a very thin* specimen area that is susceptible to hydrogen pickup associated with TEM specimen preparation after irradiation, but does not occur in a thicker specimen area.
6. The hydrogen content (H/V) in the ordered bct structure is estimated to be approximately $H/V = 0.24$. This content is much lower than $H/V \sim 0.41$, the lowest content of the β_1 hydride phase that can exist in the thermoequilibrium state, supporting the absence of hydride formation in the bct phase.

Acknowledgements

The authors would like to express their gratitude to Drs Y. Aono, R. Ishibashi and H. Arakawa, Hitachi Research laboratory, Hitachi, Ltd., for their help with use of HIP apparatus, and to Professor. H. Matsui, IMR, Tohoku University, and Dr S. Matsuo for his valuable comments on the paper.

References

[1] R.J. Kurtz, K. Abe, V.M. Chernov, D.T. Hoelzer, H. Matsui, T. Muroga, G.R. Odette, J. Nucl. Mater. 329–333 (2004) 47.

[2] T. Muroga, T. Nagasaka, K. Abe, V.M. Chernov, H. Matsui, D.L. Smith, Z.-Y. Xu, S.J. Zinkle, J. Nucl. Mater. 307–311 (2002) 547.
[3] T. Muroga, M. Gasparotto, S.J. Zinkle, Fus. Eng. Des. 61&62 (2002) 12.
[4] R.J. Kurtz, R.H. Jones, E.E. Bloom, A.F. Rowcliffe, D.L. Smith, G.R. Odette, F.W. Wiffen, Nucl. Fus. 39 (1999) 2055.
[5] S.J. Zinkle, H. Matsui, D.L. Smith, A.F. Rowcliffe, E. van Osch, K. Abe, V.A. Kazakov, J. Nucl. Mater. 258–263 (1998) 205.
[6] J.S. Benjamin, Met. Trans. 1 (1970) 2943.
[7] T. Kuwabara, H. Kurishita, M. Hasegawa, J. Nucl. Mater. 283–287 (2000) 611.
[8] H. Kurishita, T. Kuwabara, M. Hasegawa, S. Kobayashi, K. Nakai, J. Nucl. Mater. 343 (2005) 318.
[9] T. Kuwabara, H. Kurishita, M. Hasegawa, Mater. Sci. Eng. A 15 (2006) 16.
[10] H. Kurishita, T. Kuwabara, M. Hasegawa, Mater. Sci. Eng. A 433 (2006) 32.
[11] H. Kurishita, T. Kuwabara, M. Hasegawa, Mater. Sci. Eng. A, in press.
[12] S. Kobayashi, Y. Tsuruoka, K. Nakai, H. Kurishita, Mater. Trans. 45 (2004) 29.
[13] S. Kobayashi, Y. Tsuruoka, K. Nakai, H. Kurishita, J. Nucl. Mater. 329–333 (2004) 447.
[14] S. Oda, H. Kurishita, Y. Tsuruoka, S. Kobayashi, K. Nakai, H. Matsui, J. Nucl. Mater. 329–333 (2004) 462.
[15] H. Kurishita, S. Oda, S. Kobayashi, K. Nakai, T. Kuwabara, M. Hasegawa, J. Nucl. Mater., submitted for publication.
[16] T. Sakamoto, H. Kurishita, S. Kobayashi, K. Nakai, H. Arakawa, H. Matsui, Mater. Trans., in press.
[17] H. Asano, M. Hirabayashi, 2nd Inter. Congr. Hydrogen Met. (1977) 1D6.
[18] H. Asano, Y. Abe, M. Hirabpayashi, Acta Metall. 24 (1976) 95.
[19] K. Hiraga, H. Ikeda, H. Hirabayashi, J. Appl. Phys. 19 (1980) 397.